

Interactions of Organophosphorous Agents with Water and Components of Polyelectrolyte Membranes

Supporting Information

Ming-Tsung Lee, Aleksey Vishnyakov, Gennady Yu. Gor, Alexander V. Neimark

In the supporting information, we explained the details of experiments and computations in the main text. Section I described technical difficulties of experiments and our procedures regarding to these issues. Section II and III aimed the justification of ideal gas assumption in COSMO*therm*. Section IV visited the similarities between G-agents and simulants, by viewing their surface charge density distribution.

I. Experimental procedure to measure the Vapor-Liquid Equilibrium

Calibration: The compositions of the equilibrium vapor and liquid phases were obtained via interpolation of the density and refraction index of the liquid and the distillate onto reference curves $\rho(x)$ and $n_D(x)$ obtained as follows. Liquid DMMP of 99.5% purity was obtained from Pfaltz & Bauer and used as purchased. We made 15 reference solution samples of approximately 10 ml each with different liquid compositions, including pure water and pure DMMP. Due to the fact that mixing DMMP and water is exothermic, samples for calibration curve were prepared in 15 ml sealed vials and left in the exhaust hood overnight until the temperature stabilized to hood temperature $23.9\pm 0.1^\circ\text{C}$ before measurements. Refractive index and temperature of these samples were measured by Vee Gee PDX-95 digital refractometer. The prism assembly of the refractometer was cleaned by distilled water and blew dried by air during each measurement. Refractive index for 1.0 ml of solution was then measured with 4 digits accuracy. Data of refractive index is listed in Table S1, with the corresponding calibration curve plotted in Figure S1. The density calibration curve $\rho(x)$ was measured in a similar fashion: we made 21 samples of approximately 20ml each and measured the densities by DMA 35N, a specific gravity meter from Anton Paar. Densities of 0.9975 g/cm^3 and 1.1571 g/cm^3 at 24°C were obtained for water and DMMP, correspondingly. The experimental densities of mixtures exceed the densities of corresponding ideal mixtures throughout the entire concentration range, indicating a strongly hydrophilic solvation. Experimental values for the densities and excess molar volumes of DMMP—water binary mixtures have been published recently¹.

Distillation: To measure liquid and vapor composition under equilibrium temperatures, 200 ml of DMMP—water solution was placed in the still pot of Othmer still distillation column. A flexible small diameter fiberglass heating cords from Cole-Parmer, attached to the circulation leg in the bottom of the still pot, was used as a heating element. The heating rate was controlled by variable autotransformer (type 3 PN 1010) from Staco Energy. Temperature was monitored using Acorn Temp 6 RTD thermometer and temperature probe. To increase the rate of distillation and to stabilize the temperature within the bottle, still pot was insulated by fiberglass cloth stuffed with insulating foam. As soon as the temperature stabilized around a constant value and a continuous flow of condensed vapor was established, we assumed that the vapor-liquid equilibrium has been reached. The distillate from the collector was removed at that moment, and

a new collection was started. As soon as about 10 ml of the distillate was collected, the distillate and a sample of the pot liquid were placed in vials, which were kept in the hood overnight to reach the hood temperature of $24 \pm 0.2^\circ\text{C}$. The temperature was continuously monitored during the distillation process.

Table S1. Measurements for refractive index of DMMP and water binary mixtures at 24°C . V_{DMMP} and V_{water} represent volume of pure solvent used in preparing sample solution, and x_{DMMP} is the corresponding mole fraction of DMMP. Measured refractive index of DMMP is denoted as nD . $T(^{\circ}\text{C})$ -prism is the prism temperature shown on the refractometer. Temperature deviation in our measurement is at maximum 0.2 degree to the target temperature 24.0°C , which brings a negligible deviation on refractive index to the 4th digit.

| Sample | V_{DMMP} [ml] | V_{water} [ml] | x_{DMMP} | nD | $T(^{\circ}\text{C})$-prism |
|---------------|--|---|-------------------------------------|------------------------|---|
| 1 | 10.00 | 0.00 | 1.000 | 1.4130 | 23.8 |
| 2 | 20.00 | 0.10 | 0.971 | 1.4128 | 23.9 |
| 3 | 14.00 | 0.10 | 0.959 | 1.4127 | 23.8 |
| 4 | 14.00 | 0.21 | 0.918 | 1.4123 | 23.9 |
| 5 | 10.00 | 0.21 | 0.889 | 1.4120 | 23.9 |
| 6 | 5.50 | 0.21 | 0.815 | 1.4111 | 23.9 |
| 7 | 4.50 | 0.30 | 0.716 | 1.4097 | 23.9 |
| 8 | 5.00 | 0.50 | 0.628 | 1.4082 | 23.9 |
| 9 | 5.00 | 0.80 | 0.513 | 1.4058 | 23.9 |
| 10 | 5.00 | 1.10 | 0.434 | 1.4032 | 23.9 |
| 11 | 5.00 | 1.80 | 0.319 | 1.3975 | 23.9 |
| 12 | 5.00 | 3.00 | 0.219 | 1.3885 | 23.9 |
| 13 | 5.00 | 5.00 | 0.144 | 1.3775 | 24.0 |
| 14 | 5.00 | 9.00 | 0.086 | 1.3650 | 23.9 |
| 15 | 0.00 | 10.00 | 0.000 | 1.3331 | 23.9 |

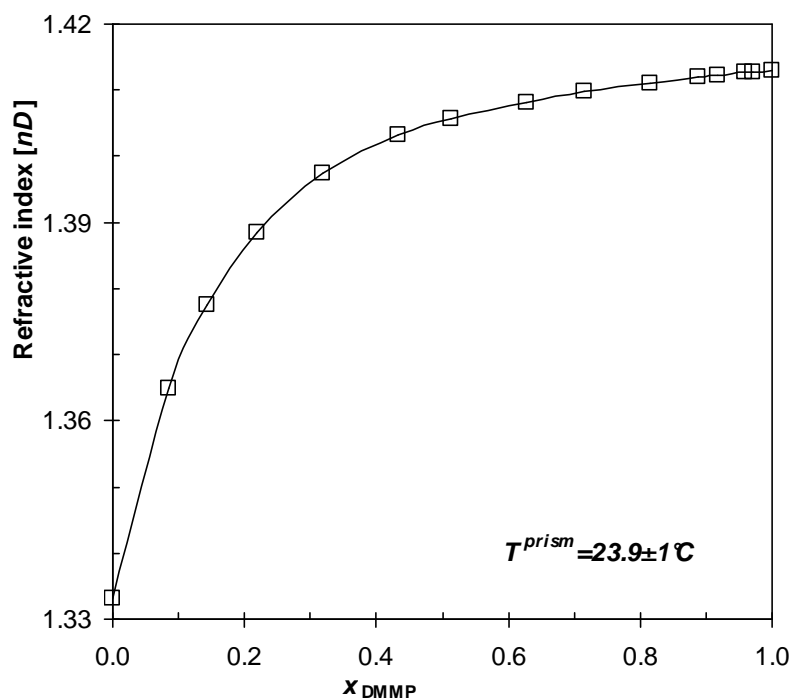


Figure S1. Measured dependence of the refractive index of solution on the composition of DMMP-water mixture at 24°C used as a calibration curve.

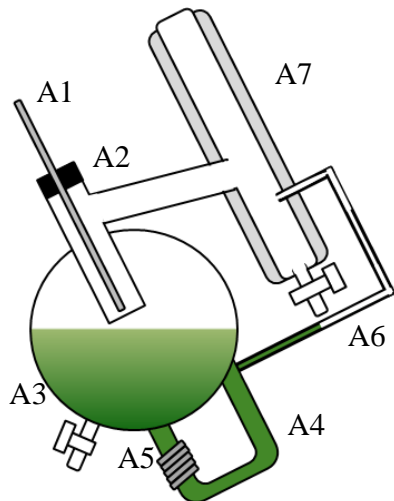


Figure S2. Distillation setup for identifying equilibrium temperatures of solutions with fixed liquid phase composition. Apparatus: A1 - thermometer probe, A2 - rubber cap, A3 - still pot, which attached to A4 - circulation leg, which is heated by heating cords (A5). A6 is the reflux system of the still bottle, and A7 is the cooling pipe. If the apparatus is tilted as shown here, all condensed vapor flows back to the still bottle. When the apparatus is in the upright position, the distillate is collected in the collector. For low-pressure distillations, a vacuum pump is connected to the top of cooling pipe.

Technical issues and our refinements: We encountered several difficulties during our experiment. At P=1atm. The boiling temperatures of the solutions are high enough to make hydrolysis problem during the distillation. The hydrolysis was signified by an appearance of boiling during in the process of initial heating, unstable temperature during the distillation, and unreasonable vapor curve. NMR experiment (Figure S3) confirmed a substantial amount of methanol in the distillate and DMMP decomposition products in the pot liquid. The equation of the main reaction presumably is

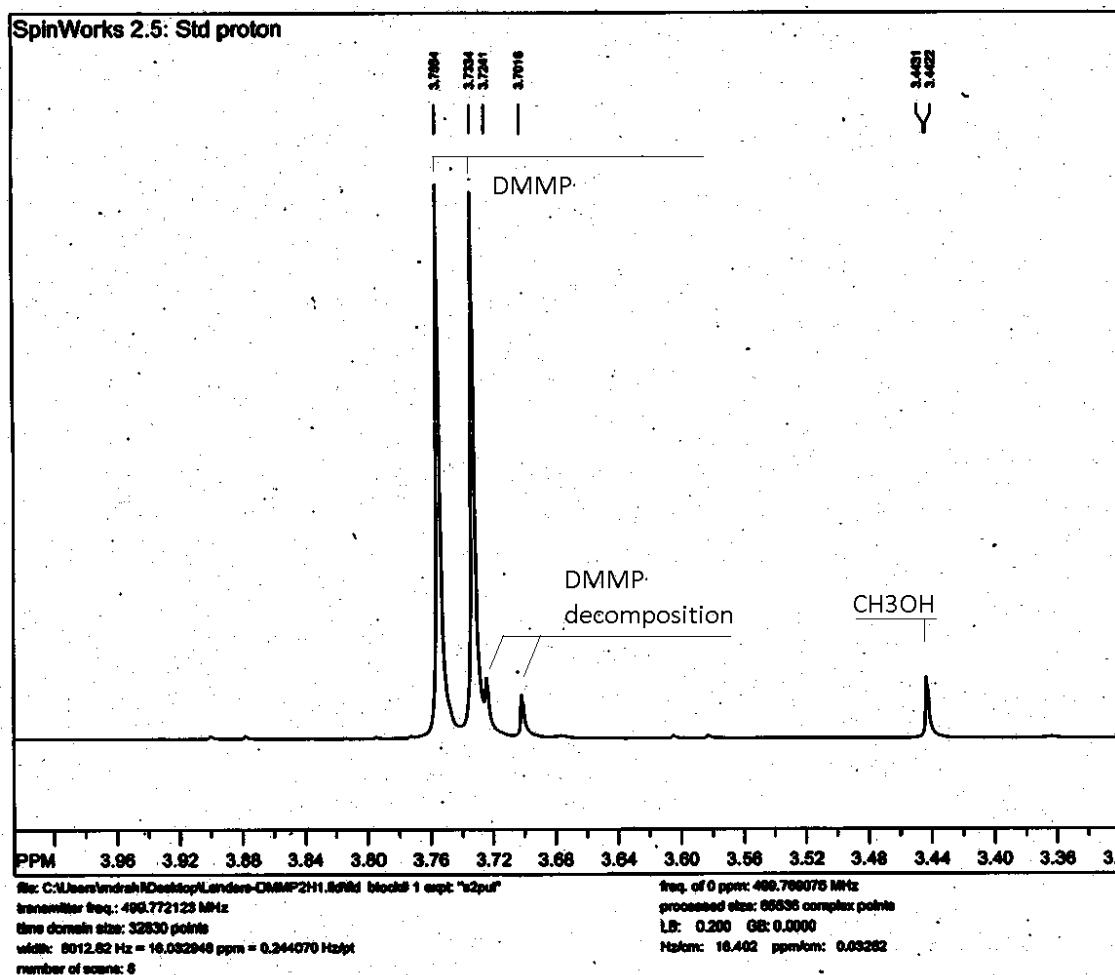
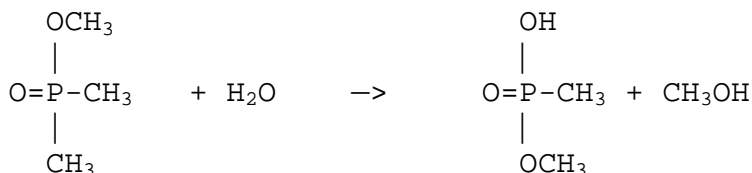


Figure S3. Proton NMR spectrum of the distillate sample obtained at 1 atm. Operating temperature is approximately at 130 to 150°C.

Not all decomposition products were identified. For this reason, we explored only the boiling temperature dependence on the composition (the liquid line) and discarded the vapor line. However, by lowering the pressure we brought the boiling temperature down and avoided hydrolysis. No condensed vapor was observed below the equilibrium temperature at the pressures of 0.226 and 0.311 atm, and the distillate samples showed no peaks for hydrolysis products. In viewing VLE phase diagram (Figure 3 in the text), one may concern the lack of vapor phase experimental data for y_{DMMP} larger than 0.3, and the reason refers to another difficulty in our experiments. It was related to a steep dependence of the boiling temperature on composition. Since the concentration of water in the distillate is much larger than in the liquid, the concentration constantly changes in the process of the experiment. Although its effect is negligible in water-rich solutions, it is substantial in DMMP-rich solutions. In a few instances, the temperature was never stabilized, despite the reflux system in our column. It can be exemplified using one of our experiments at 0.23. We had a bottle of solution made of 200 ml of DMMP and only 2.9 ml of water; liquid phase mole fraction of DMMP is about 0.92. Based on our measurements and COSMO-RS calculations, vapor phase composition of DMMP is about 0.3 at equilibrium. For reaching the minimum amount of the requirement for refractometer, we took 1 ml of distillate. This made the composition of liquid phase become 0.95, and it raised the equilibrium temperature by 9 degrees (from 107 to 116°C). However, we also need a certain amount of distilled vapor to flush the cooling pipe before collecting the distillate for measurement, which raised the liquid composition and the equilibrium temperature even higher. For these DMMP-rich solutions, only the liquid curve was measured by our modification (Figure S2), which directed the distillate back into the pot in order to keep the composition of the pot liquid constant. The equilibrium temperatures were observed stabilized within the ± 1 degree.

(a)

P=1atm

| T(°C) | x_{DMMP} | Dev-T |
|-------|------------|-------|
| 100.8 | 0.000 | 0.0 |
| 101.1 | 0.059 | 0.2 |
| 101.4 | 0.077 | 0.1 |
| 101.6 | 0.111 | 0.1 |
| 103.5 | 0.405 | 1.0 |
| 113.0 | 0.709 | 0.8 |
| 120.6 | 0.803 | 0.3 |
| 130.6 | 0.860 | 1.6 |
| 139.0 | 0.924 | 1.4 |
| 147.7 | 0.961 | 1.4 |
| 180.4 | 1.000 | 0.1 |

(b)

P=0.311 atm

| T(°C) | x_{DMMP} | Dev-T | T(°C) | y_{DMMP} | Dev-T |
|-------|------------|-------|-------|------------|-------|
| 71.1 | 0.100 | 0.4 | 71.8 | 0.016 | 0.4 |
| 71.9 | 0.200 | 1.1 | 72.5 | 0.029 | 0.2 |
| 73.1 | 0.300 | 0.9 | 74.5 | 0.027 | 1.0 |
| 75.0 | 0.400 | 2.0 | 74.7 | 0.024 | 1.0 |
| 79.5 | 0.500 | 0.4 | 76.7 | 0.040 | 0.9 |
| 81.2 | 0.627 | 2.0 | 79.5 | 0.038 | 1.0 |
| 83.3 | 0.639 | 1.4 | 81.2 | 0.072 | 2.0 |
| 83.8 | 0.663 | 2.0 | 83.8 | 0.072 | 2.0 |
| 84.2 | 0.669 | 1.0 | 84.2 | 0.059 | 1.0 |
| 86.5 | 0.651 | 2.0 | 93.2 | 0.093 | 0.9 |
| 93.2 | 0.815 | 0.9 | 96.6 | 0.106 | 1.0 |
| 96.6 | 0.823 | 1.0 | 96.7 | 0.141 | 0.0 |
| 96.7 | 0.856 | 0.0 | 98.5 | 0.195 | 2.0 |
| 98.5 | 0.840 | 2.0 | 103.1 | 0.176 | 0.7 |
| 103.1 | 0.865 | 0.7 | 104.7 | 0.164 | 0.2 |
| 104.7 | 0.918 | 0.2 | 107.9 | 0.216 | 0.1 |
| 107.9 | 0.939 | 0.1 | | | |

(c)

P=0.226 atm

| T(°C) | x_{DMMP} | Dev-T | T(°C) | y_{DMMP} | Dev-T |
|-------|------------|-------|-------|------------|-------|
| 63.0 | 0.000 | 0.0 | 68.0 | 0.015 | 2.0 |
| 65.1 | 0.144 | 0.4 | 70.8 | 0.030 | 2.0 |
| 66.1 | 0.252 | 0.1 | 71.3 | 0.035 | 2.0 |
| 67.2 | 0.347 | 0.4 | 77.1 | 0.085 | 1.6 |
| 69.0 | 0.447 | 0.4 | 85.0 | 0.165 | 2.0 |
| 71.1 | 0.543 | 0.6 | 92.0 | 0.185 | 2.0 |
| 74.5 | 0.647 | 1.8 | 104.0 | 0.320 | 2.0 |
| 77.2 | 0.743 | 1.9 | | | |
| 85.0 | 0.830 | 2.0 | | | |
| 92.0 | 0.870 | 2.0 | | | |
| 104.0 | 0.960 | 2.0 | | | |
| 132.8 | 1.000 | 0.0 | | | |

Table 2. Measurements for Vapor liquid equilibrium of DMMP and water binary mixtures at (a) 1 atm, (b) 0.311 atm and (c) 0.226 atm. The corresponding phase diagram is plotted in Figure 3 with COSMO-RS prediction. Equilibrium temperature is observed at the average temperature T(°C) with the deviation Dev-T. Maximum deviation in our measurement is set to 2 degree (i.e. ± 1). x_{DMMP} and y_{DMMP} represent liquid phase and vapor phase composition at the equilibrium temperature, by using the calibration data in Table S.1 and Figure S.1.

II. Describing VLE in DMMP-water system using Peng-Robinson cubic equation of state.

We attempted to fit our results with the Peng-Robinson (PR) equation of state (EOS). Unlike the COSMO-RS, which is designed to yield the liquid phase activity coefficients while the vapor phase is considered independently, PR describes both liquid and vapor with the same EOS:

$$P = \frac{RT}{\underline{V} - b(\underline{x})} - \frac{a(T, \underline{x})}{\underline{V}^2 + 2b(\underline{x})\underline{V} - b(\underline{x})^2} \quad (1)$$

For pure component, $a(T, \underline{x})$ and $b(\underline{x})$ are function of the critical properties.

$$a_i(T) = 0.45724 \frac{R^2 T_{c,i}^2}{P_{c,i}} \alpha_i(T) \quad (2)$$

$$b_i = 0.07780 \frac{RT_{c,i}}{P_{c,i}} \quad (3)$$

with $\sqrt{\alpha_i(T)} = 1 + \kappa_i (1 - \sqrt{T/T_{c,i}})$ and $\kappa_i = 0.37464 + 1.54226\omega_i - 0.26992\omega_i^2$, where ω_i is the acentric factor of species i .

For mixtures, $a(T, \underline{x})$ and $b(\underline{x})$ are pseudo one-fluid parameters and can be determined using mixing rules. Here we used the van der Waals one fluid mixing rule (eq. 4, 5) with standard combining rules (eq. 6) listed below:

$$a(T, \underline{x}) = \sum_i \sum_j x_i x_j a_{ij} \quad (4)$$

$$b(\underline{x}) = \sum_i x_i b_i \quad (5)$$

$$a_{ij} = \sqrt{a_i a_j} (1 - k_{ij}) \quad (6)$$

Adjustable parameter k_{ij} in eq. 6 describes interactions between the molecules of different components and is usually fitted to binary experimental data.

The equilibrium liquid and vapor compositions at given temperature and pressure were calculated using a standard iterative procedure (see e.g. ²).

Parameter evaluation: The critical properties of DMMP are not known, but were estimated by Sokkalingam et al ³ in their classical Monte Carlo simulations. We decided to rely on the reported experimental properties namely the saturated vapor pressures ⁴ and liquid densities at 0, 25 and 100 °C⁵⁻⁷. The best fit we obtained corresponded to $T_c = 685.6$ K and $P_c = 46.1$ atm, which is somewhat lower compared to $T_c = 700.6$ K and $P_c = 49.05$ atm reported by Sokkalingam et al ³. Acentric factor was taken from Sokkalingam et al with the value 0.39.

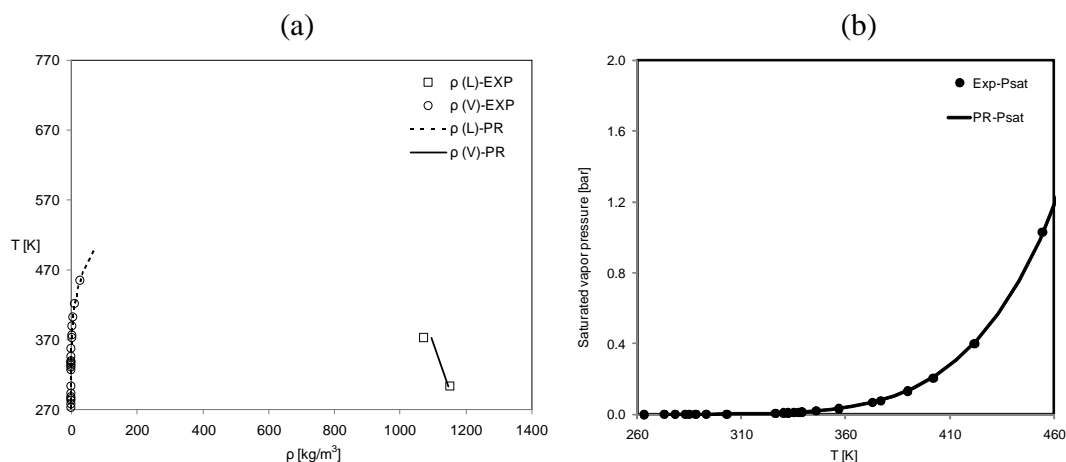


Figure S4. Single-component Peng-Robinson EOS fit to the experimental properties of pure DMMP. (a) densities: squares represent experimental liquid densities of DMMP, and solid line is fitted by PR EOS. Circles are experimental vapor densities, which are calculated by experimental saturated pressures using ideal gas law (b) saturated vapor pressures of experiments (circles) and the fitting of PR EOS (line).

We attempted to reproduce our experimental VLE diagrams with the PR EOS treating k_{ij} as a temperature-dependent fully adjustable parameter. The results are presented in Figure S5. The PR EOS reproduces VLE reasonably, though by no means exactly, despite the adjustable mixing parameter. The adjustable coefficients are slightly negative (0.12 for 0.226 and 0.311 atm, and is -0.05 for 1 atm) indicating very favorable interactions between DMMP and water.

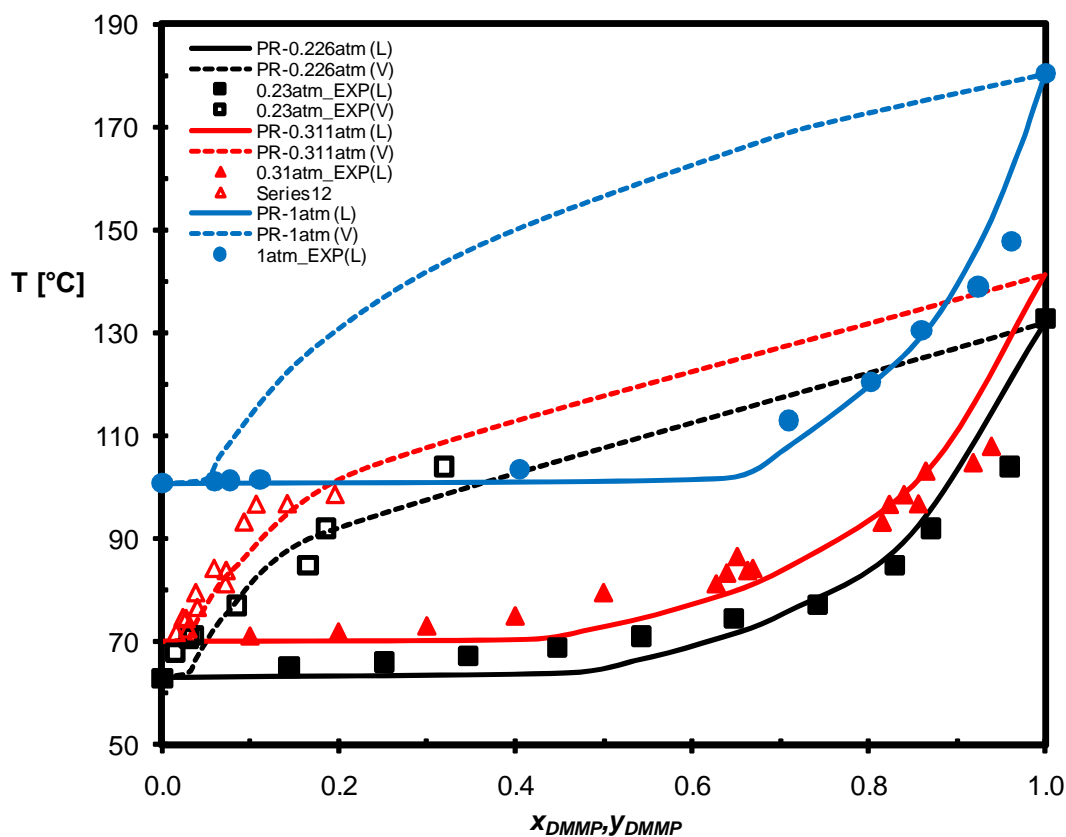


Figure S5. Experimental VLE diagrams (symbols) at $p = 0.226$ (black), 0.311 (red) and 1.0 atm (blue) modeled using the Peng-Robinson EOS (lines). Open symbols and dashed lines show the vapor curves; closed symbols and solid lines show the liquid curves. Adjustable parameter is -0.12 for 0.226 and 0.311 atm, and is -0.05 for 1 atm.

III. Examination of vapor phase nonideality – Using PR EOS to correct the DMMP-water VLE diagrams obtained by COSMO-RS

In our VLE calculations (Figure 3) using *COSMOtherm*, ideal behaviour of the gas phase is assumed. Knowing the critical properties of DMMP and water, we use PR EOS combined with the COSMO-RS to examine the ideal gas assumption. The results of this correction at $P = 1$ atm are presented in Figure S6. It is clear that the difference is smaller than the statistical error of the experimental results. The ideal gas assumption in *COSMOtherm* VLE calculation is valid for systems at 1 atm and below.

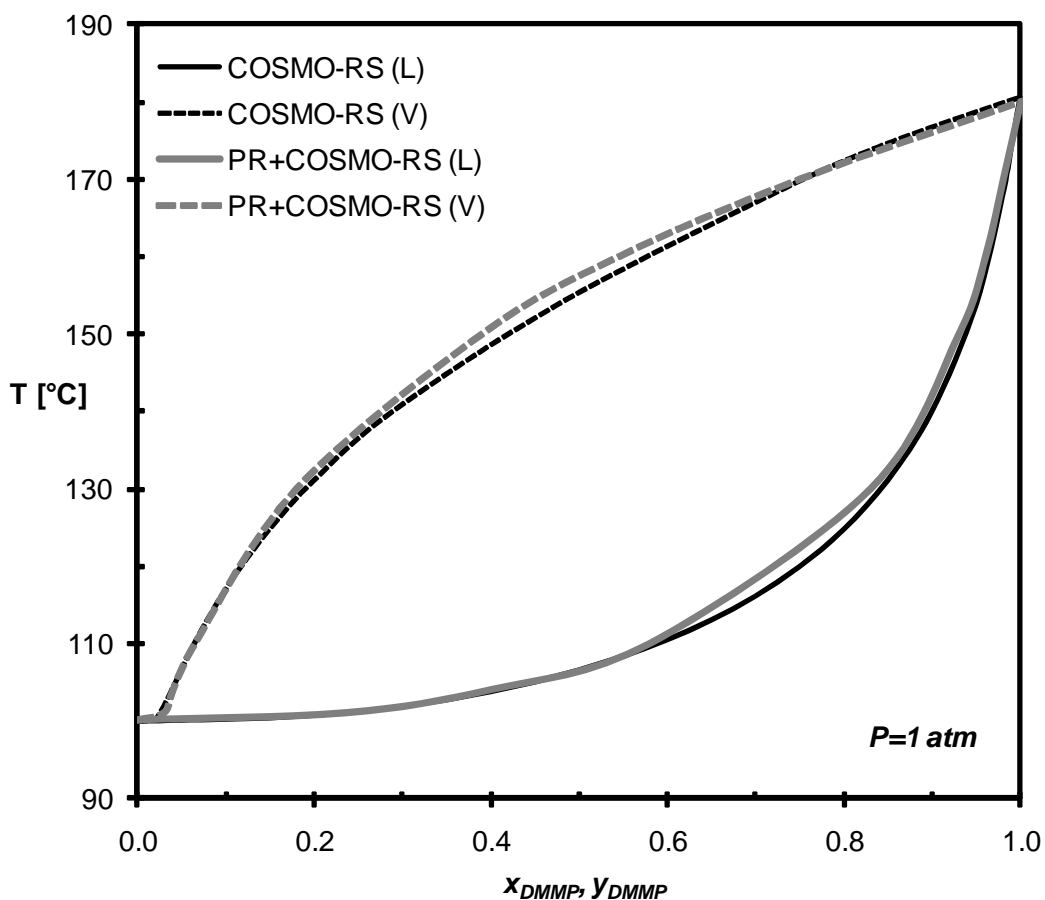


Figure S6. VLE diagrams at 1 atm for water-DMMP binary mixture calculated using COSMO-RS activity coefficients for the liquid phase and ideal gas (black lines) as well as Peng-Robinson (gray lines) equation of state for the equilibrium vapor.

IV. σ profile of G-agents and the stimulants used in COSMO-RS calculations

The following figure is the charge density distribution for DMMP, DIFP, sarin and soman, obtained from PQS ab-initio. σ profile of DIFP is similar to that of soman in size and shape, and so do the profiles of DMMP and sarin. The stronger hydrophilicity of DMMP than sarin can also be observed by the stronger polarization in the σ profile.

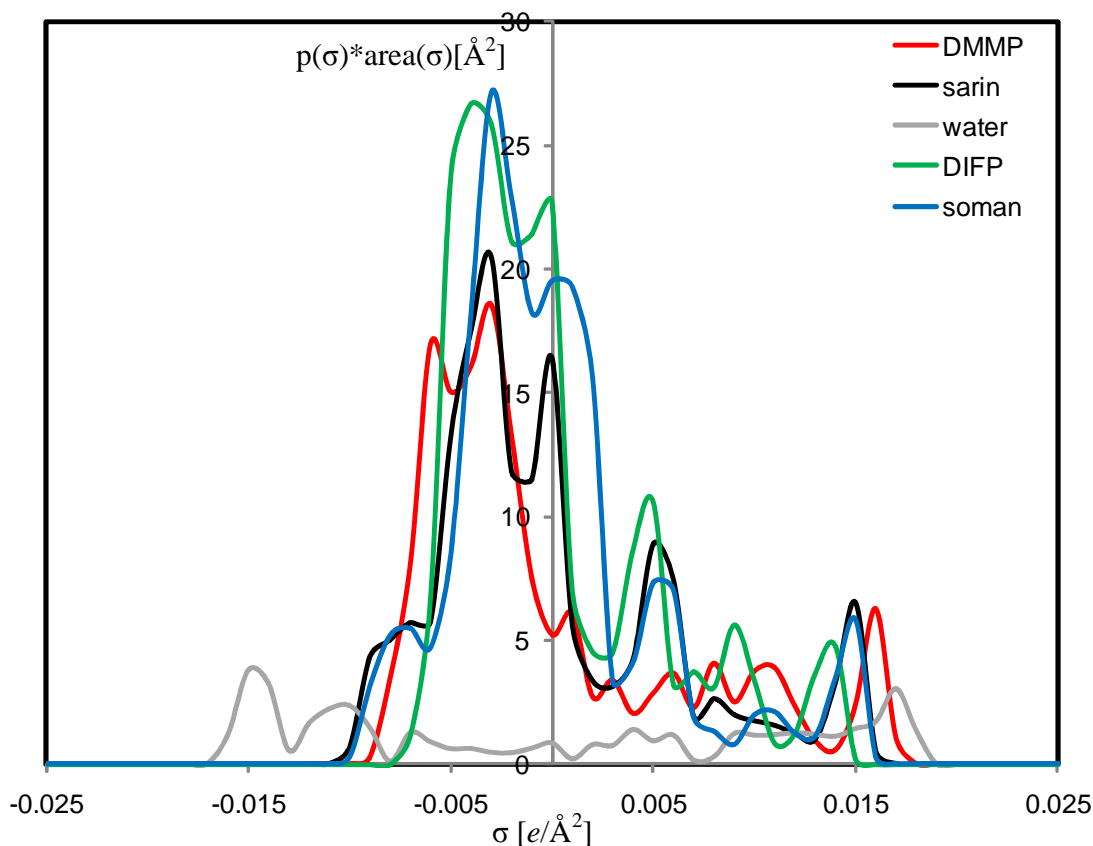


Figure S7. σ -profiles (area versus charge density) for DMMP, DIFP, sarin and soman. y-axis is the probability times area, and x-axis is charge per unit area.

References

- (1) Vishnyakov, A.; Gor, G. Y.; Lee, M.-T.; Neimark, A. V. *The Journal of Physical Chemistry A* **2011**, *115*, 5201.
- (2) Elliott, J. R.; Lira, C. T. *Introductory chemical engineering thermodynamics*; Prentice Hall PTR: NJ, 1999.
- (3) Sokkalingam, N.; Kamath, G.; Coscione, M.; Potoff, J. J. *Journal of Physical Chemistry B* **2009**, *113*, 10292.
- (4) Butrow, A. B.; Buchanan, J. H.; Tevault, D. E. *Journal of Chemical and Engineering Data* **2009**, *54*, 1876.
- (5) Kosolapoff, G. M. *Journal of the Chemical Society* **1954**, 3222.
- (6) Kosolapoff, G. M. *Journal of the American Chemical Society* **1954**, *76*, 615.
- (7) Bartelt-Hunt, S. L.; Knappe, D. R. U.; Barlaz, M. A. *Critical Reviews in Environmental Science and Technology* **2008**, *38*, 112.